
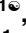




RESEARCH ARTICLE

Novel EBV LMP-2-affibody and affitoxin in molecular imaging and targeted therapy of nasopharyngeal carcinoma

Shanli Zhu¹ , Jun Chen¹ , Yirong Xiong¹ , Saidu Kamara¹, Meiping Gu¹, Wanlin Tang¹, Shao Chen¹, Haiyan Dong¹, Xiangyang Xue¹, Zhi-Ming Zheng^{2*}, Lifang Zhang^{1*} 

1 Institute of Molecular Virology and Immunology, Department of Microbiology and Immunology, School of Basic Medical Sciences, Wenzhou Medical University, Wenzhou, Zhejiang, PR China, **2** Tumor Virus RNA Biology Section, RNA Biology Laboratory, Center for Cancer Research, National Cancer Institute, National Institutes of Health, Frederick, Maryland, United States of America

 These authors contributed equally to this work.

* zhengt@exchange.nih.gov (ZMZ); wenzhouzlf@126.com (LZ)



 OPEN ACCESS

Citation: Zhu S, Chen J, Xiong Y, Kamara S, Gu M, Tang W, et al. (2020) Novel EBV LMP-2-affibody and affitoxin in molecular imaging and targeted therapy of nasopharyngeal carcinoma. *PLoS Pathog* 16(1): e1008223. <https://doi.org/10.1371/journal.ppat.1008223>

Editor: Fanxiu Zhu, Florida State University, UNITED STATES

Received: June 18, 2019

Accepted: November 18, 2019

Published: January 6, 2020

Copyright: This is an open access article, free of all copyright, and may be freely reproduced, distributed, transmitted, modified, built upon, or otherwise used by anyone for any lawful purpose. The work is made available under the [Creative Commons CC0](https://creativecommons.org/licenses/by/4.0/) public domain dedication.

Data Availability Statement: All relevant data are within the manuscript and its Supporting Information files.

Funding: LZ has received funding from the National Natural Science Foundation of China [grant number:81372447, 81972550](<http://www.nsf.gov.cn>). ZMZ was supported by Intramural Research Program of the NCI Center for Cancer Research, NIH. The funders had no role in study design, data collection and analysis, decision to publish, or preparation of the manuscript.

Abstract

Epstein-Barr virus (EBV) infection is closely linked to several human malignancies including endemic Burkitt's lymphoma, Hodgkin's lymphoma and nasopharyngeal carcinomas (NPC). Latent membrane protein 2 (LMP-2) of EBV plays a pivotal role in pathogenesis of EBV-related tumors and thus, is a potential target for diagnosis and targeted therapy of EBV LMP-2⁺ malignant cancers. Affibody molecules are developing as imaging probes and tumor-targeted delivery of small molecules. In this study, four EBV LMP-2-binding affibodies ($Z_{EBV\ LMP-2\ 12}$, $Z_{EBV\ LMP-2\ 132}$, $Z_{EBV\ LMP-2\ 137}$, and $Z_{EBV\ LMP-2\ 142}$) were identified by screening a phage-displayed LMP-2 peptide library for molecular imaging and targeted therapy in EBV xenograft mice model. $Z_{EBV\ LMP-2}$ affibody has high binding affinity for EBV LMP-2 and accumulates in mouse tumor derived from EBV LMP-2⁺ xenografts for 24 h after intravenous (IV) injection. Subsequent fusion of *Pseudomonas* exotoxin PE38KDEL to the $Z_{EBV\ LMP-2\ 142}$ affibody led to production of Z142X affitoxin. This fused Z142X affitoxin exhibits high cytotoxicity specific for EBV⁺ cells *in vitro* and significant antitumor effect in mice bearing EBV⁺ tumor xenografts by IV injection. The data provide the proof of principle that EBV LMP-2-specific affibody molecules are useful for molecular imaging diagnosis and have potentials for targeted therapy of LMP-2-expressing EBV malignancies.

Author summary

Molecular imaging diagnosis and targeted therapy have been successfully used for several types of tumors, but not yet applied to diagnose or treat EBV-associated NPC. Affibody molecules are small proteins engineered to bind to a large number of target proteins with high affinity, and therefore, can be developed as potential biopharmaceutical drugs for molecular diagnosis and therapeutic applications. In the present study, we screened and characterized EBV LMP-2-specific affibodies and evaluated their usage in molecular imaging of LMP-2 expressing cells and EBV LMP-2 tumor-bearing mice. Subsequently,

Competing interests: The authors have declared that no competing interests exist.

we engineered and obtained an EBV LMP-2 affitoxin based on EBV LMP-2-binding affibodies and demonstrated its targeted cytotoxicity for EBV⁺ cell lines *in vitro* and *in vivo*. Our data indicate that the EBV LMP-2-specific affibody and its derived affitoxin are useful for diagnosis of LMP-2 expressing cells and targeted therapy of EBV-derived, LMP-2⁺ malignancies.

Introduction

Epstein-Barr virus (EBV) is a γ -herpesvirus that primarily infects human B cells and epithelial cells and establishes a lifelong persistent, asymptomatic infection within peripheral memory B cells [1, 2]. Like other members of the herpesvirus family, the life cycle of EBV can switch between latent and lytic state. Latent EBV infection leads to several malignancies, including endemic Burkitt's lymphoma, Hodgkin's lymphoma, nasopharyngeal carcinomas (NPC) and gastric carcinoma [2, 3]. Recently, more attention has been drawn to the relation of EBV infection with NPC. Molecular epidemiological and serological studies have revealed the important etiological role of EBV in NPC carcinogenesis. Almost 100% of sera from undifferentiated and poorly differentiated NPC patients have high-titre antibodies to EBV antigens, and almost all of undifferentiated NPC tumor cells carry EBV genome and express EBV viral proteins [4–7].

Latent EBV genome expresses six EBV-encoded nuclear antigens (EBNA-1, -2, -3A, -3B, -3C and LP), and two membrane proteins (latent membrane proteins LMP-1 and LMP-2) [2]. Depending on the gene expression profile, the EBV latency can be grouped into type I, II, and III [8]. In the B-cells that are infected and transformed by EBV, both LMP-1 and LMP-2 are expressed only in type II and III latencies along with all other latent genes. LMP-1 is a major viral oncoprotein and is essential for the oncogenic process which drives B-cell transformation *in vitro* [9–11]. The LMP-2 gene expresses two alternative isoforms, LMP-2A and LMP-2B which contain 9 exons. However, the exon 1 of LMP-2A and LMP-2B is transcribed separately from two different promoters, but both exon 1 can be spliced in frame to exon 2 [12]. The LMP-2A exon 1 has the coding function, but the LMP-2B exon 1 does not. Thus, LMP-2B utilizes an initiation methionine codon in the exon 2 for its translation and is thus a smaller protein (378 aa residues) than LMP-2A (497 aa residues). Consequently, both forms of LMP-2 are almost identical except for the presence of an additional 119 amino acid residues in the N-terminus of LMP-2A which forms a cytoplasmic domain [13]. Although both forms of LMP-2 have 12 transmembrane domains [13], the cytoplasmic domain of LMP-2A bears several motifs including eight tyrosine residues and regulates the activities of protein tyrosine kinases (Syk and Lyn). Thus, LMP-2A could block tyrosine phosphorylation induced by B-cell receptor (BCR) to prevent activation of lytic EBV replication and to maintain EBV latency [14,15]. Furthermore, LMP-2A supports LMP-1 functions to some extent and contributes to the malignant transformation of the host cells by intervening with signalling pathways at multiple points, especially in the apoptotic and cell cycle pathway [16]. LMP-2B colocalizes with LMP-2A and prevents the switch from latent to lytic EBV replication [17,18]. Therefore, LMP-2 is an ideal target for diagnosis and targeted therapy of EBV LMP-2⁺ malignancies.

Affibody molecules are a class of small (58 amino acids, ~6.5 kDa), non-immunoglobulin affinity proteins that contain a Z domain derived from staphylococcal protein A [19]. By combinational randomization of amino acid residues within helices I and II of the three-helical bundle of the Z-domain scaffold, large libraries can be constructed, from which potent binders for theoretically any given target [20] can be isolated by a variety of display methods. Rapid tumor localization, fast clearance from blood and nonspecific compartments make affibody

molecules attractive for many medical applications, including *in vivo* molecular imaging, receptor signal blocking and delivery of toxin [21,22]. To date, over 400 published studies show that affibody molecules have been selected for targeting more than 40 different proteins and served as affinity moieties in a variety of applications [22]. The affibody-targeted proteins include epidermal growth factor receptor (EGFR) [23,24], human epidermal growth factor receptor 2 (HER2) [25,26], human epidermal growth factor receptor 3 (HER3) [27,28], vascular endothelial growth factor (VEGF) [29], and human papillomavirus type 16 E7 (HPV16E7) [30,31]. In particular, affibody molecules attached with a cytotoxin appear to be a straightforward and efficient way to direct the action of the toxin to desired cell targets [22].

In the present study, we screened and characterized EBV LMP-2-binding affibody molecules and evaluated their usage in molecular imaging in tumor-bearing mice. Subsequently, we prepared the EBV LMP-2 affitoxin based on EBV LMP-2-binding affibody proteins and investigated further the targeted cytotoxicity for EBV LMP-2⁺ cell lines *in vitro* and *in vivo*. Our data concluded that the EBV LMP-2-specific affibody and affitoxin molecules can be used for imaging diagnosis of LMP-2⁺ cells and have potentials for targeted therapy of EBV-derived, LMP-2⁺ NPC. To our knowledge, this is the first report that EBV-specific affibody as a novel probe used for *in vivo* imaging diagnosis of the EBV LMP-2⁺ tumors. Most importantly, our study provides the first evidence that EBV LMP-2-specific affitoxin is a novel agent useful for inhibiting the growth of EBV LMP-2⁺ tumor.

Results

Screening and selection of four LMP-2-binding affibody molecules

A total of 282 clones interactive with EBV LMP-2 B-epitope fusion protein (S1 Fig) were selected for DNA sequencing after four rounds of phage display library screening in combination with ELISA screening for EBV LMP-2 binding activity at 0.45 μ M in 100 μ l/well (S2 Fig). 69 clones (69/282 or 24.5%) possess the correct sequence, bearing a total of 13 randomized amino acid residues in helices 1 and 2 of the Z domain when compared to the original affibody scaffold molecule Z_{WT}. Moreover, there is no premature termination codon in these randomized sequences. Four potential affibody molecules: Z_{EBV LMP-2}12 (GenBank accession No. MH807659, denoted as Z12), Z_{EBV LMP-2}132 (GenBank accession No. MH807660, denoted as Z132), Z_{EBV LMP-2}137 (GenBank accession No. MH807661, denoted as Z137) and Z_{EBV LMP-2}142 (GenBank accession No. MH807662, denoted as Z142), which showed the best binding to EBV LMP-2 in the subsequent ELISA screenings, were selected for further studies. The 13 randomized amino acid residues of the four affibody molecules are presented in S3 Fig. The gene fragments of the four affibody molecules were then subcloned into pET21a (+) vector in frame with a C-terminal His-tag. The expressed affibody proteins in *E. coli* were purified by Ni-NTA agarose resin. SDS-PAGE analysis showed that the molecular weight is about 6.5 kDa and the final products were approximately in 95% of purity, which was used for subsequent investigations (Fig 1A).

The selected affibodies bind to recombinant LMP-2 with high affinity

Surface plasmon resonance (SPR) biosensor assay was performed to verify the binding affinity of the selected affibodies to the target protein EBV LMP-2. The affibody molecules were injected at different concentrations over the flow-cell surface of a chip containing immobilized recombinant EBV LMP-2 B-epitope fusion protein. The SPR results showed a concentration-dependent increase in resonance signals for each analysed affibody in binding to LMP-2, indicating that the four affibodies selected from our phage display library screening bind directly to LMP-2 in a dose-dependent manner (Fig 1B–1E), whereas the unselected original affibody

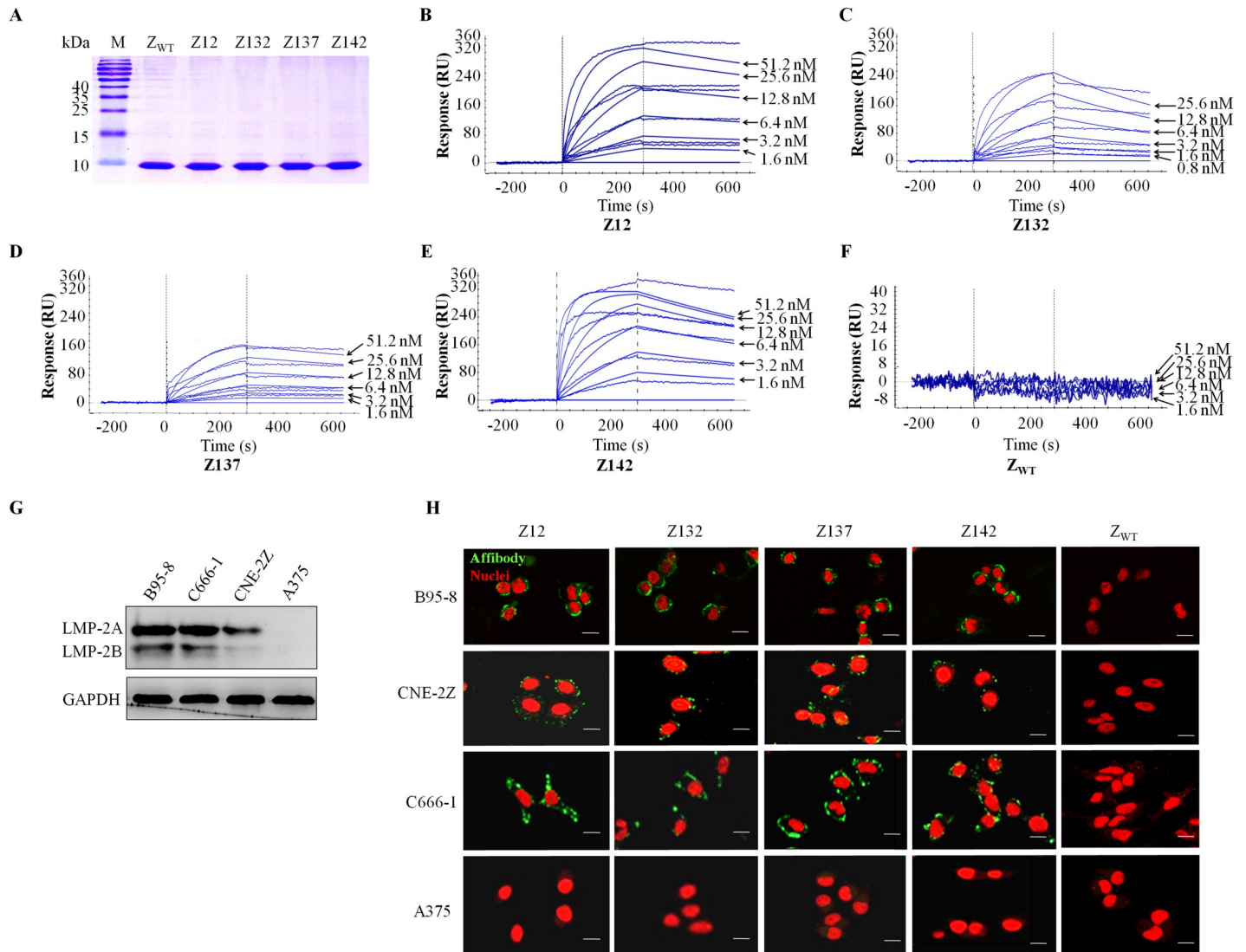


Fig 1. The selected 4 affibody molecules bind to recombinant and native EBV LMP-2. (A) SDS-PAGE analysis showed that the molecular weight of affibody is about 6.5 kDa, which is in consistency with expected size, and the purity of the final products is about 95%. M, protein ladder. (B-F) Biosensor assays. Representative binding sensorgrams showing the interaction of affibodies with immobilized recombinant EBV LMP-2 B-epitope fusion protein. Binding of 1.6, 3.2, 6.4, 12.8, 25.6, 51.2 nM of Z12, Z137, Z142, and an unselected original affibody scaffold molecule Z_{WT} (B, D, E, F) and 0.8, 1.6, 3.2, 6.4, 12.8, 25.6 nM of Z132 (C) to LMP-2 on the sensorchip was analysed by a SPR-based binding assay. Sensorgrams was obtained after injection of the Z_{EBVLMP-2} affibodies over an EBV LMP-2 flow-cell surface at selected concentrations. Two independent experiments were performed and Z_{WT} without binding affinity to EBV LMP-2 at all concentrations served as a negative control. (G) LMP-2 expressions in EBV⁺ cell lines. Western blot analysis was conducted for LMP-2 expression in B95-8, C666-1 and CNE-2Z cell lines. A375 cell line served as the EBV-negative control. Rabbit serum against EBV LMP-2 B-epitope fusion protein was used as a primary antibody (prepared-in-house). (H) Fluorescence staining of EBV⁺ cells with the selected four affibodies. FITC-conjugated goat anti-mouse IgG served as the secondary antibody, and mouse anti-His mAb was used to detect the His-tagged affibody molecules (green). EBV⁺ B95-8, CNE-2Z and C666-1 cells and EBV-negative melanoma A375 cells were used for comparative staining with individual affibody molecules. The unselected original affibody scaffold molecule Z_{WT} with no binding affinity to LMP-2 served as a control. Cell nuclei were counterstained with PI (red). Scale bar, 20 μm.

<https://doi.org/10.1371/journal.ppat.1008223.g001>

scaffold molecule Z_{WT} showed no LMP-2 B-epitope fusion protein binding activity (Fig 1F), nor the Z142 to an unrelated protein MAGE-A3 (S4 Fig). Further calculations revealed that the dissociation equilibrium constants (KD) of Z12, Z132, Z137 and Z142 affibodies were 1.45×10^{-6} mol/L, 3.74×10^{-6} mol/L, 3.90×10^{-6} mol/L, 1.14×10^{-6} mol/L, respectively (S1 Table). These SPR data indicated that the selected four affibodies bind to recombinant EBV LMP-2 B-epitope fusion protein with high affinity.

The selected affibodies interact with native LMP-2 protein in EBV⁺ cells

To evaluate the interaction of selected affibodies with native LMP-2, we first examined the expression of LMP-2 in EBV⁺ B95-8, C666-1 and CNE-2Z cell lines by Western blot using a rabbit anti-serum against EBV LMP-2 B-epitope fusion protein prepared in-house as a primary antibody. As shown in Fig 1G, we demonstrated that our rabbit antibody against the LMP-2 B-epitope fusion protein which was used in our phage display library screening could recognize LMP-2 by Western blot and the expression of LMP-2 in B95-8 and C666-1 were slightly higher than that in CNE-2Z. Given that the affibody molecules selected in this study were able to bind to recombinant LMP-2 B-epitope fusion protein in SPR biosensor analysis, we next investigated whether the selected four LMP-2-binding affibodies could also bind to native LMP-2 protein in EBV⁺ cells using an indirect immunofluorescence assay (IFA). Since the linear LMP-2 epitopes used in our phage display screening were positioned outside of the LMP-2 transmembrane region from the C-terminal LMP-2, the selected affibodies would be useful for detection of both LMP-2A and LMP-2B from the EBV⁺ cells with both type II and III latencies. As shown in Fig 1H, EBV⁺ B95-8, C666-1 and CNE-2Z cells expressing LMP-2 were all positive for four LMP-2-binding affibody staining with bright green fluorescence signals on the cell membrane. As expected, there was no visible staining in the cells incubated with the unselected original affibody scaffold molecule Z_{WT}. Similarly, no fluorescence signal was observed in EBV-negative melanoma A375 cells when the cells were incubated separately with each affibody (Fig 1H). The LMP-2 membrane staining profile by four LMP-2-binding affibodies can be confirmed by a rat anti-LMP-2A monoclonal antibody (mAb) (Fig 2A). Extended incubation time of Z142 affibody with C666-1 cells up to 6 hours would not change the membrane LMP-2 staining status (Fig 2B). Confocal immunofluorescence co-localization assay confirmed that the fluorescence signals of LMP-2 and Z142 were co-localized in C666-1 cells (Fig 2C). These data indicated that all four affibodies did specifically bind to native membrane LMP-2 in EBV⁺ cells.

Biodistribution of the selected LMP-2 affibodies and their accumulation in mouse EBV tumor xenografts by binding to native LMP-2

To confirm further the biodistribution and *in vivo* tumor-targeting ability of LMP-2-specific affibody proteins, nude mice bearing C666-1 tumor xenografts were intravenously injected with Dylight755-labeled Z_{EBV LMP-2} affibody (15.4 nmol in 100 μl PBS per mouse) or an equal amount of unselected affibody scaffold molecule Z_{WT} and then scanned using an NIR (near-infrared) imaging system at different time points after injection. As shown in Fig 3, fluorescence signal of Dylight755-Z_{EBV LMP-2} affibody molecules in subcutaneous C666-1 tumor xenografts were detectable at 0.5 h post-injection. Subsequently, the fluorescence intensity in the tumor gradually increased until 4–6 h post-injection and then decreased gradually. The fluorescence signal of Z137 and Z142 at tumor sites persisted for at least 48 h. In addition, affibody accumulation in the kidneys was observed because the small size of affibody proteins are cleared via renal filtration. As expected, no tumor-specific fluorescence signal was observed in the xenografts in the mice injected with Dylight755-labeled Z_{WT} (Fig 3). These results indicated that Z_{EBV LMP-2} affibodies bind specifically to the C666-1-derived tumour. Since the resident time of the Z142 affibody in the mouse body appeared much longer than that of other three Z_{EBV LMP-2} affibodies, the Z142 was subsequently selected as a vehicle to deliver cytotoxin to LMP-2⁺ tumours.

Engineered Z142X binds to native EBV LMP-2 with high specificity

The toxin part used in this study was a truncated fragment of *Pseudomonas* exotoxin (PE38 toxin). The C-terminal part of the PE38 was optimized to a KDEL (Lys-Asp-Glu-Leu)

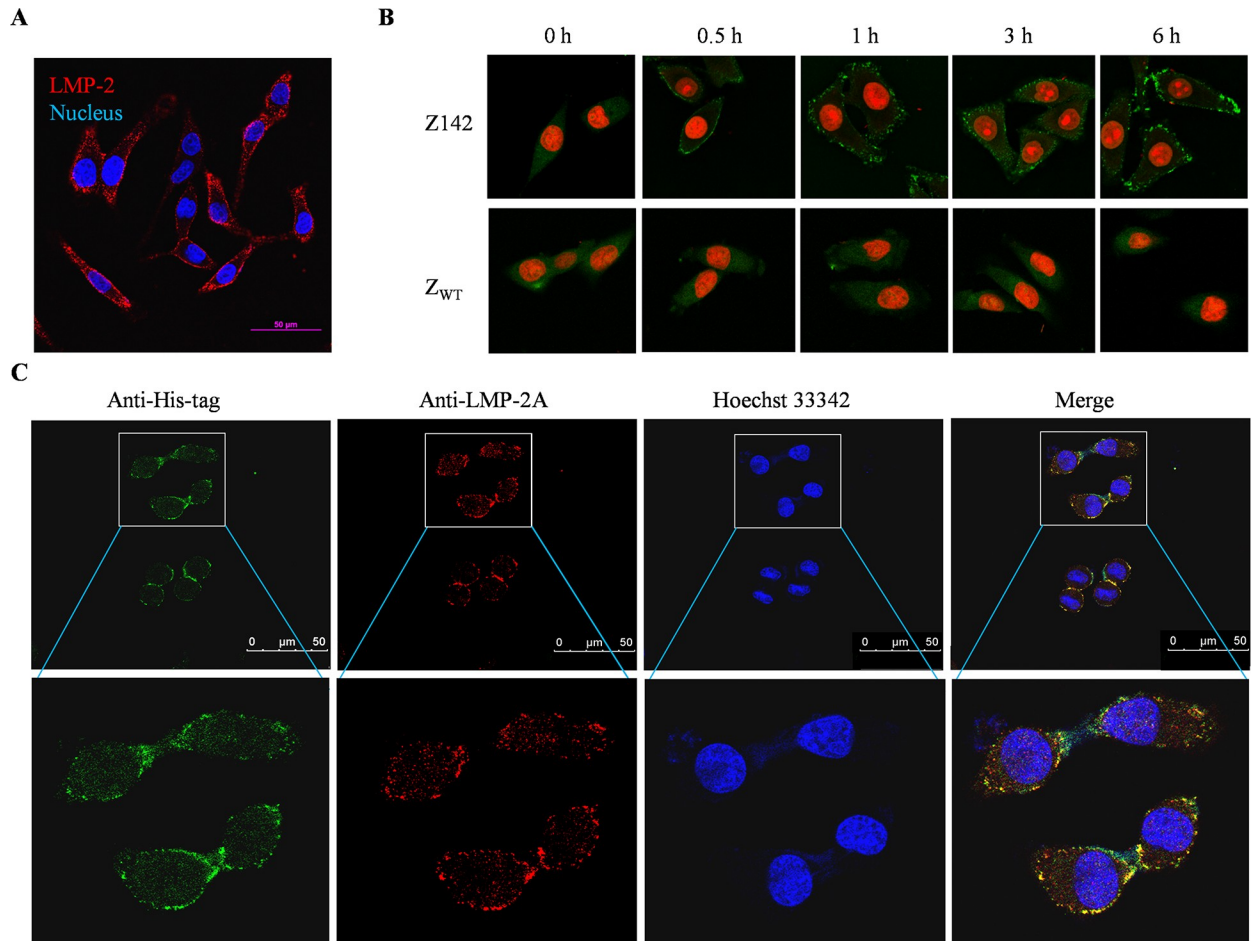


Fig 2. Z142 affibody and rat anti-LMP-2A mAb recognize the same native membrane-bound LMP-2 expressed in NPC-derived EBV⁺ C666-1 cells. (A) Membrane LMP-2 staining profile of C666-1 cells by IFA using a rat anti-LMP-2A mAb. (B) Constant binding of Z142-His affibody to membrane LMP-2 expressed in C666-1 cells was examined by anti-His-tag IFA at the indicated incubation time (hr) of the Z142 affibody. (C) Representative Z142-His affibody (green) and anti-LMP-2A (red) co-staining of native membrane-bound LMP-2 expressed in C666-1 cells. The cell nuclei were stained by Hoechst 33342 (blue). The merged images showed the LMP-2 specific co-staining (yellow). Scale bar, 50 μ m.

<https://doi.org/10.1371/journal.ppat.1008223.g002>

sequence to increase the exotoxin cytotoxicity [32,33] and the optimized exotoxin PE38KDEL-based immunotoxins have been approved for clinical trials by the US FDA [34]. To produce the toxin fusion protein of Z142, affitoxin Z142X, PE38KDEL was genetically fused to the C-terminus of Z142 affibody (Fig 4A). The unselected affibody scaffold molecule Z_{WT} served as a control fusion. The recombinant plasmids of pET21a (+)/Z_{EBV LMP-2} affitoxin142 (Z142X) and pET21a (+)/Z_{WT} affitoxin (Z_{WT}X) were constructed and confirmed by sequencing. Z142X and Z_{WT}X expressed in *E. coli* BL21 (DE3) were purified using Ni-NTA affinity chromatography. As shown in Fig 4B, the purified Z142X and Z_{WT}X were visualized as a single protein band on SDS-PAGE gel by Coomassie brilliant blue staining, as well as by Western blot with a His-tag mAb. The protein bands at 45 kDa were detected in consistency with the expected sizes of Z142X and Z_{WT}X.

The binding affinity of Z142X at a dose of 5.56 nM to LMP-2 B-epitope fusion protein (1 nmol) was verified by SPR biosensor assay, showing a much higher resonance signal for Z142X, whereas Z_{WT}X appeared no binding to EBV LMP-2 B-epitope fusion protein in the assay (Fig 4C). When compared with Z142 at the similar dose in the binding assay (Fig 1E), we

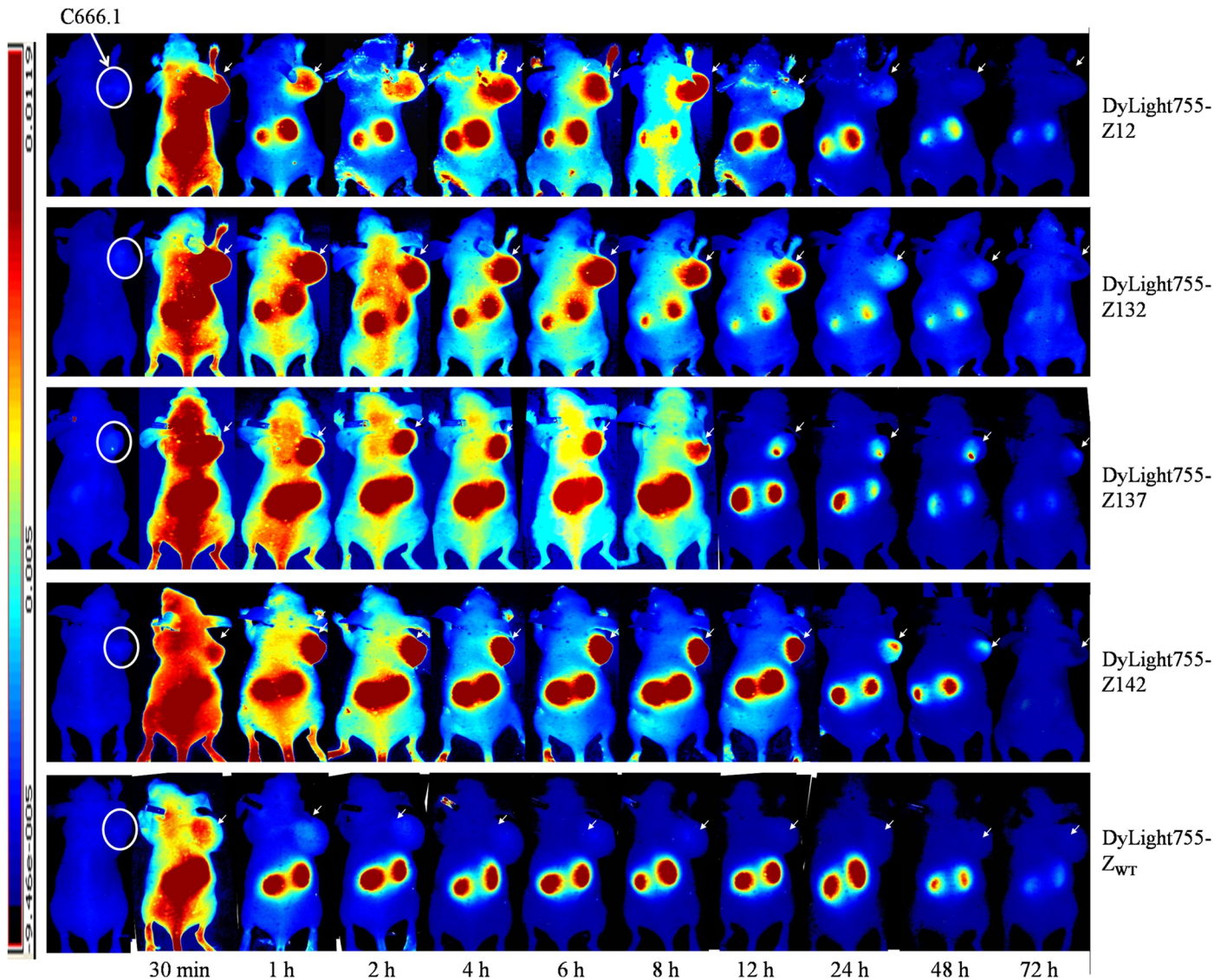


Fig 3. Tumor uptake of the affibody molecules by subcutaneous xenografts. Mice bearing C666-1 xenografts (circles) were intravenously injected with DyLight755-labeled affibody molecules followed by dynamic scanning with *in vivo* NIR system. The unselected original affibody scaffold molecule Z_{WT} with no binding affinity to LMP-2 served as a control. The fluorescence signal in xenografts were detectable at 0.5 h post-injection. Subsequently, the fluorescence intensity in the tumor gradually increased until 4–6 h post infection and then decreased gradually. The fluorescence signal of Z137 and Z142 at tumor sites persisted for at least 48 h. In addition, affibody accumulation in the kidneys was observed because the small size of affibody proteins are cleared via renal filtration. No tumor-specific fluorescence signal was observed in the xenografts in the mice injected with DyLight755-labeled Z_{WT} molecules.

<https://doi.org/10.1371/journal.ppat.1008223.g003>

did not see any notable effect on LMP-2 B-epitope fusion protein binding by addition of PE38KDEL to the affibody Z142.

To assess the binding specificity of Z142X to native LMP-2 expressed in cells, EBV⁺ B95-8, C666-1 and CNE-2Z cells and EBV-negative A375 cells was examined by IFA. The mouse anti-His mAb, rabbit SPA-Z polyclonal antiserum and mouse PE38KDEL polyclonal antiserum were used respectively as the primary antibody. Cells incubated with $Z_{WT}X$ served as negative controls. As shown in Fig 4D, when B95-8, C666-1 and CNE-2Z cells were incubated with Z142X, all three primary antibodies were found to recognize the Z142X, with distribution of the fluorescence signals predominantly on the cell membrane (green) (Fig 4D). No visible

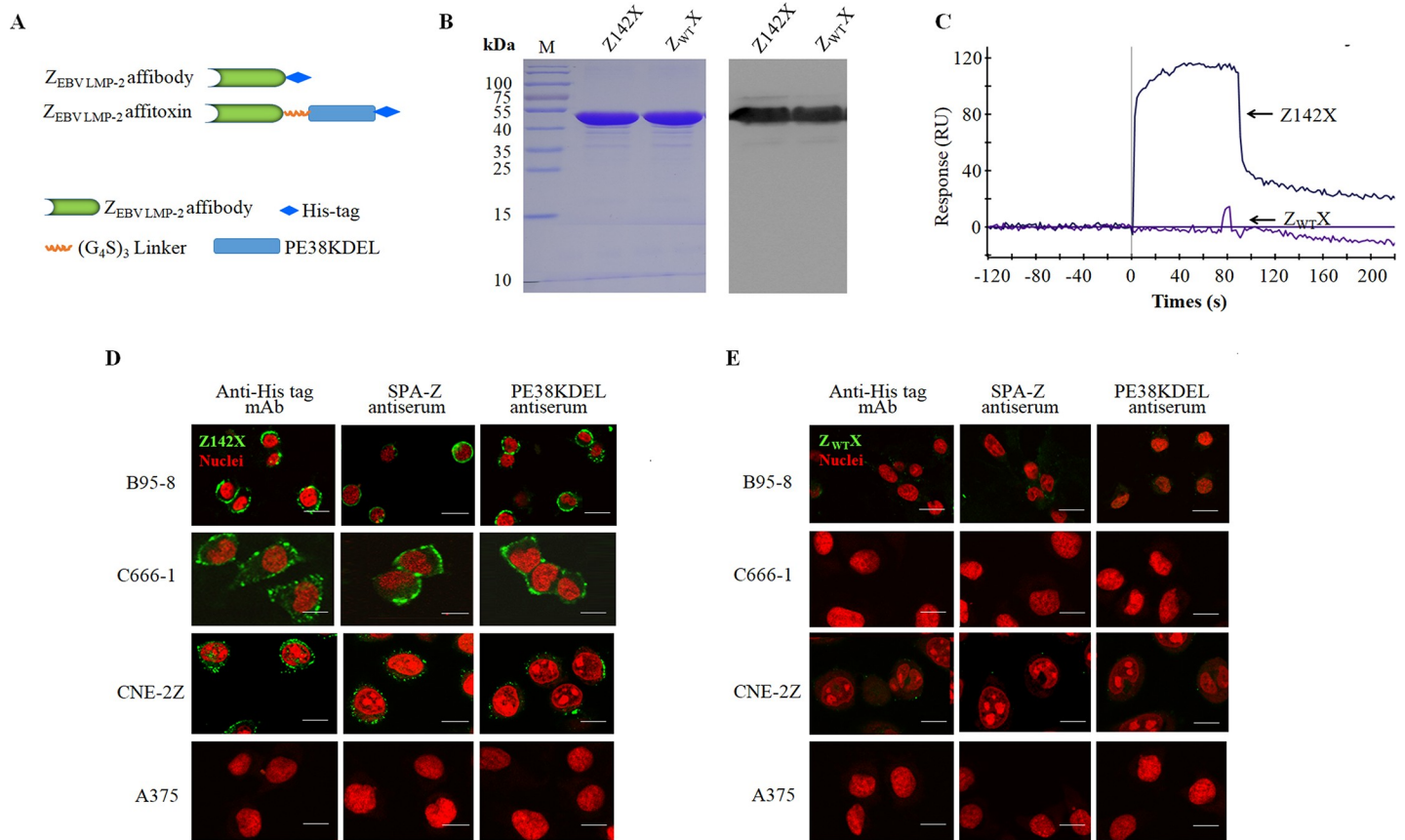


Fig 4. Engineered Z142X affitoxin binds to native EBV LMP-2 with high specificity. (A) Schematic structures of Z142X affitoxin. (B) SDS-PAGE Coomassie blue staining (left panel) and Western blot (right panel) analysis of purified Z142X and Z_{WT}X. In Western blot assay, anti-His mAb was served as primary antibody. (C) Biosensor assays. Representative binding sensor grams show the interaction of affitoxin molecules (5.56 nM) with immobilized recombinant LMP-2 B-epitope fusion protein (1 nmol). (D & E) Fluorescence staining of EBV⁺ B95-8, C666-1 and CNE-2Z cells with Z142X (D) or unselected original affibody scaffold molecule Z_{WT}X (E). The Z_{WT}X affitoxin with no binding affinity to LMP-2 served as a control. Mouse anti-His mAb, rabbit SPA-Z polyclonal antiserum and mouse PE38KDEL polyclonal antiserum were used respectively as a primary antibody. FITC-conjugated goat anti-mouse IgG and goat anti-rabbit IgG were used as the secondary antibodies (green). EBV-negative melanoma A375 cells labelled with the same Z142X molecules served as control cells. Cell nuclei were counterstained with PI (red) (600×). Scale bar, 20 μm.

<https://doi.org/10.1371/journal.ppat.1008223.g004>

signal was observed when B95-8, C666-1, and CNE-2Z cells when incubated with Z_{WT}X (Fig 4E). Similar negative results were also obtained when EBV-negative A375 cells were incubated with Z142X (Fig 4D). Based on these results, we conclude that fusion PE38KDEL to the Z142 affibody did not interfere with the EBV LMP-2-binding ability of affibody.

Cytotoxicity of Z142X affitoxin on EBV⁺ cells

The cytotoxicity of Z142X, Z142, Z_{WT}X and PE38KDEL on B95-8 cells at 0.07, 0.14, 0.28, 0.56, 1.11, and 2.22 μM was initially evaluated on EBV⁺ B95-8 cells by CCK-8 kit. We found that the viability of B95-8 cells was decreased along increasing concentration of Z142X and Z142, with Z142X being more toxic than Z142 as expected; whereas Z_{WT}X and PE38KDEL displayed only a little or no effect on B95-8 cell viabilities at the tested doses (S5 Fig). Subsequently, two additional EBV⁺ cell lines C666-1 and CNE-2Z and an EBV-negative A375 cell line were included for the treatment with different concentrations of Z142X affitoxin and Z_{WT}X and the cell viabilities were then examined by using a CCK-8 kit. The viability of B95-8, C666-1 and CNE-2Z cells decreased along increasing concentrations of Z142X (S6 Fig). Further calculations

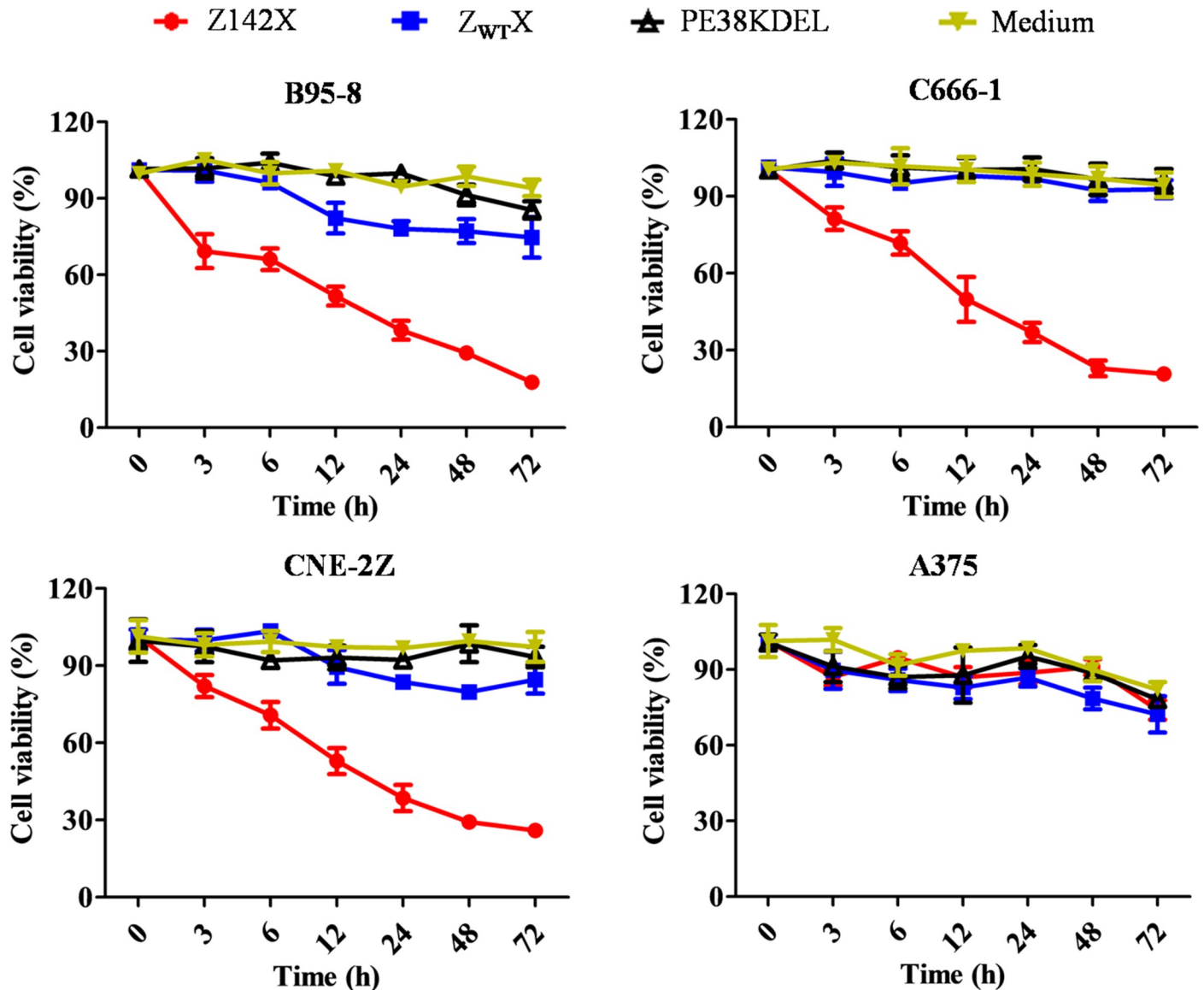


Fig 5. Z142X specifically kills EBV⁺ cells *in vitro*. EBV⁺ cells (B95-8, C666-1 and CNE-2Z) and EBV-negative cell (melanoma A375 cell) in 96-well plate were treated with 2.22 μM of Z142X or control agents (Z_{WT}X, PE38KDEL and medium) for the indicated time. Cell viability was assessed by using CCK-8 Kit. 2.22 μM of Z142X reduced significantly the viability of EBV⁺ cells (B95-8, C666-1 and CNE-2Z) during the indicated time periods, whereas A375 cells treated with the same concentration of Z142X remained fully viable. The control agents (Z_{WT}X, PE38KDEL and medium) had no effect on any cell lines.

<https://doi.org/10.1371/journal.ppat.1008223.g005>

revealed that the IC₅₀ values of Z142X at 72 hours were $0.313 \pm 0.054 \mu\text{M}$ for B95-8 cells, $0.412 \pm 0.063 \mu\text{M}$ for C666-1 cells and $0.453 \pm 0.139 \mu\text{M}$ for CNE-2Z cells. Thus, the highest concentration of 2.22 μM was chosen for further investigation. The cytotoxicity of Z142X was then assessed in different time periods (0, 3, 6, 12, 24, 48 and 72 h). As shown in Fig 5, Z142X at 2.22 μM reduced significantly the viability of EBV⁺ cells (B95-8, C666-1 and CNE-2Z) during the indicated time periods, whereas A375 cells treated with the same concentration of Z142X remained fully viable. As expected, Z_{WT}X, which has no binding to EBV LMP-2, had no effect on any cell lines (Fig 5). The results indicate that PE38KDEL fusion to the Z142 affibody exhibits PE38KDEL cytotoxic activity and did not affect Z142X's binding to native EBV LMP-2 in EBV⁺ cells.

***In vivo* acute toxicity of Z142X affitoxin**

The toxicity of Z142X was assessed in BALB/c mice by intravenous tail vein injection at the indicated concentrations. As listed in [S2 Table](#), mice injected with 667 nmol/kg and 556 nmol/kg of the Z142X protein were all dead at 72 h post-injection in all three experiments. One of the tested mice survived with the treatment of 444 nmol/kg in the experiment I and experiment III. Three and two of tested mice survived with treatment of 333 nmol/kg also in the experiment II and III, respectively, whereas only two of the tested mice were dead in all three experiments at 222 nmol/kg. Accordingly, the calculated LD50 value was 264.8 nmol/kg at 72 h post-injection. Subsequently, 100 nmol/kg of Z142X was chosen for the following anti-EBV tumour studies, although Z142X at 55.6 nmol did induce two animals died in one of three experiments.

Z142X affitoxin inhibits tumour growth in mice bearing EBV tumours

The antitumor effect of Z142X affitoxin was evaluated in mice bearing C666-1 and CNE-2Z xenografts. Tumor cells were subcutaneously injected into mice as described in Materials and methods section. When the tumor sizes reached to 50~100 mm³, the mice were administrated with equal amounts of Z142X, Z142, Z_{WTX}, PE38KDEL or PBS every two days for 15 times via tail vein. As shown in [Fig 6A–6C](#), from day 0 to day 15, the C666-1 tumour sizes in all groups increased slowly. By day 15 and after, the average tumor sizes increased rapidly in the control groups, while the tumor in the Z142X affitoxin- or Z142 affibody-treated animals displayed remarkable growth inhibition. At the end of this experiment, we did not see any animal died from the treatment regimen in the course of observation and the average tumour weights of PBS-, PE38KDEL-, Z_{WTX}-, Z142- and Z142X-treated mice were 4.35±0.51, 4.06±0.59, 3.89±0.47, 2.54±0.05 and 1.46±0.16 g, respectively. The average tumor weights in Z142X-treated animals were significantly lower than that in the control mice ($P<0.05$). Consistently in the mice bearing subcutaneous CNE-2Z tumor xenografts, Z142X affitoxin was a much stronger inhibitor than that of control agents ($P<0.05$) ([Fig 6D–6F](#)). The average tumor weights in Z142X-treated mice was 0.64±0.12 g, whereas Z142 affibody, Z_{WTX}, PE38KDEL and PBS-treated animals had tumor weights at 2.21±0.17, 3.26±0.24, 3.75±0.25, 4.28±0.23 g, respectively. Z142 affibody did exert inhibitory activity to tumour growth as a result from its slightly weaker cytotoxicity effect than that of Z142X ([S5 Fig](#)). As expected, the control agents (Z_{WTX}, PE38KDEL or PBS) did not show any anti-tumor effect on these mice ([Fig 6](#)), nor the Z142X affitoxin and Z142 affibody on tumour growth in mice bearing EBV-negative A375 tumor xenografts ([S7 Fig](#)). We also noticed that the mice treated with Z142X did not show significant weight loss and survived more than 1.5 months without any signs of organ dysfunctions. Together, our results provide the first evidence that the Z142X affitoxin might be a useful precision medicine specific for EBV⁺ tumours.

Discussion

NPC is a geographical cancer and has relatively high incidence in Southeast Asia and mainland China [35]. Like other cancers, distant metastasis and local recurrence are the leading cause of death in NPC patients. Thus, the early diagnosis and therapy of NPC plays a crucial role in preventing of metastasis. Concurrent chemotherapy and radiation therapy have significantly improved the outcome of NPC. However, the overall survival rate of NPC patients is still poor [36,37]. Therefore, it is urgent to carry out early diagnosis of NPC and effective specific molecular targeted therapy. Published data have confirmed that undifferentiated NPC is associated closely (100%) with EBV infection [38]. EBV LMP-2 is expressed in type II and III latencies to maintain the latent EBV infection and contributes to the malignant transformation by intervening with signalling pathways at multiple points, especially in the cell cycle and apoptotic

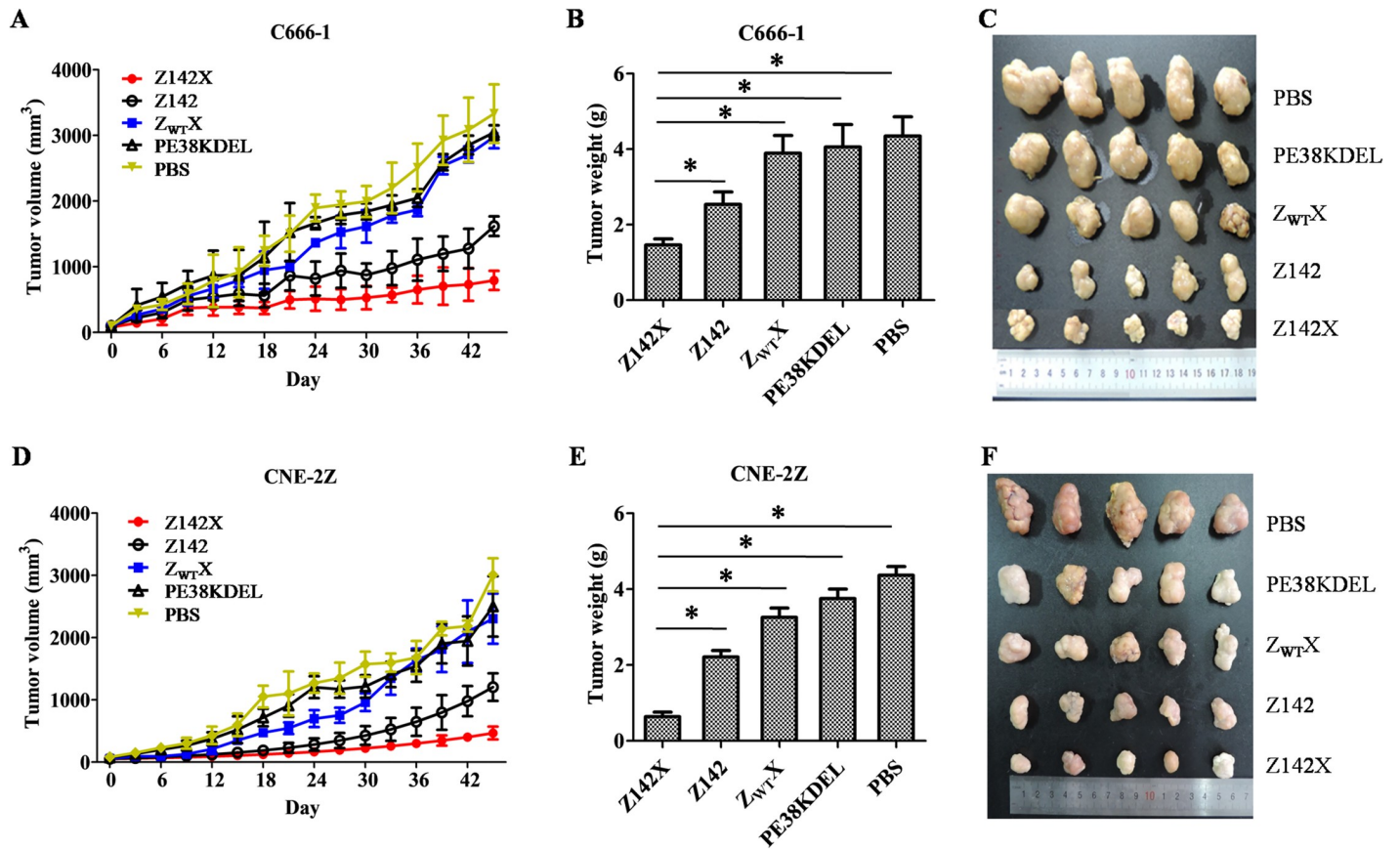


Fig 6. Z142X affitoxin prevents EBV tumor growth in mice bearing C666-1 (A-C) or CNE-2Z (D-F) tumor xenografts. Mice bearing C666-1 tumor grafts were intravenously injected with 100 nmol/kg Z142X, Z142, or an equal amount of control agents or the same volume of PBS every two days for 15 times via tail vein. Tumor growth was monitored by measuring the tumor volume every day. The average tumor sizes increased rapidly in the control groups, while the tumor in the Z142X affitoxin- or Z142 affibody-treated animals displayed remarkable growth inhibition. At the end of the experiment, all tumor grafts were removed and weighed. The average tumor weights in Z142X-treated animals were significantly lower than that in the control mice. Similar to the mice bearing subcutaneously CNE-2Z tumor xenografts, Z142X affitoxin was a much stronger inhibitor than that of control agents. Z142 affibody did exert inhibitory activity to tumor growth. The control agents (Z_{WT}X, PE38KDEL or PBS) did not show anti-tumor effect on these mice. Data represent the mean ± SD (n = 5). *P<0.05, compare to the PBS, PE38KDEL, Z_{WT}X, Z142 affibody groups. 2-tailed unpaired Student's t test was used.

<https://doi.org/10.1371/journal.ppat.1008223.g006>

pathway [14–16]. In addition, LMP-2B is colocalizing with LMP-2A and constitutively expressed primarily in the membrane of all EBV-infected cells [39, 40]. Thus, EBV LMP-2 is an ideal target for diagnosis and targeted therapy of type II/III EBV LMP-2⁺ malignant cancers.

Both molecular imaging and targeted tumor therapy are protein-based affinity tools, such as mAbs and their fragments. However, due to their large size (~150 kDa), mAbs have the inherent drawbacks of poor tissue penetration and a long residence time in circulation, which result in poor imaging contrast. Compared with mAbs, affibody molecules are very small in size (~6.5 kDa) and hence have favourable properties for diagnostic imaging and as tumor ligands for drug delivery [41]. Because of their small size, affibody can be synthesized or recombinantly expressed. Since the first construct HER2-targeting affibody molecule Z_{HER2:342} was produced and confirmed to bind to HER2-positive cancer cell lines [24], several similar affibody molecules targeting EGFR [23,24], HER3 [27,28], IGF-1R [42], HIV-1-gp120 [43] and HPV16E7 [30,31] have been reported and also applied to image several tumor-associated molecular targets, such as HER2[25, 44], EGFR[45,46], HER3[47]. The first clinical imaging study on patients with breast cancer was conducted using HER2-specific affibody, which

was labelled with ^{111}In or ^{68}Ga using both SPECT (single-photon emission computerized tomography) and PET (positron emission tomography) imaging [26,48].

Molecular imaging *in vivo* can provide a critical global view of potential metastatic lesions in cancer diagnosis and thus, has the great potential to improve the diagnosis of many diseases for appropriate treatment choices [22]. Several metabolic markers have been developed for diagnostic imaging, the most used one is ^{18}F -fluorodeoxyglucose-PET for finding the metastatic and recurrent human carcinoma. The major drawback of the technique is non-specificity of increased glucose metabolism and incapable of recognizing a cancer-specific target. PET is also costing and radioactive because its detection depends on gamma rays emitted by a positron-emitted radio ligand. The diagnosis based on molecular imaging has not been widely adopted in NPC, partly due to the lack of suitable targeting agents that have high target-binding affinity and specificity. In this study, we obtained four EBV LMP-2-specific affibodies by screening a phage display library. IFA confirmed that the affibodies specifically bind to native LMP-2 protein distributed predominately on the cell membrane of EBV⁺ cell lines. Dynamic optical imaging revealed the quickly and specifically accumulation of Dylight755- $Z_{\text{EBV LMP-2}}$ affibodies in C666-1 tumor xenografts and quick clearance from the body in this xenografts mouse model. We found that the residence time of Z142 affibody in the body was relatively longer than that of other three EBV LMP-2-binding affibodies, but the mechanism for its longer resident time in animals remains unknown.

PE38KDEL is a truncated and optimized version of PE38 and its based immunotoxins have been approved for clinical trials by the US FDA [34]. A HER2 specific affibody molecule fused to toxin PE38 could exhibit specific cytotoxicity to HER2-expressing cell [49] and inhibit growth of subcutaneous xenografts of HER2-expressing tumor cells without visible adverse effects [50]. In this report, we constructed and produced $Z_{\text{EBV LMP-2}}$ affitoxin142 (Z142X) by fusing PE38KDEL toxin to $Z_{\text{EBV LMP-2}}$ 142 affibody. As a therapeutic candidate for NPC, the Z142X must bind to its target protein, EBV LMP-2, with high specificity. We discovered that (1) the Z142X specifically interacts with native LMP-2 protein on the cell membrane of EBV⁺ cell lines and specifically identifies the xenografts derived from EBV⁺ cells; (2) the Z142X binds to LMP-2 and kills the EBV LMP-2⁺ cells, but not the EBV- negative cells; (3) the Z142X inhibits tumor growth in mice bearing NPC tumor xenografts derived from EBV⁺ C666-1 and CNE-2Z cell lines, but not melanoma xenografts (EBV-negative melanoma A375 cell line). The affibody molecule module is located on the N-terminus of affitoxin and provides LMP-2-targeting function. How the toxin part of an affitoxin gets into the target cells after the affibody part binding to the LMP-2 remains to be investigated. PE38KDEL in the cytosol was found to block protein synthesis by binding to and deactivating translation elongation factor 2 (EF-2) [51]. The finding that Z142 affibody was also fairly suppressive for the tumor growth in C666-1 and CNE-2Z xenografts implies that the LMP-2-specific affibody molecule may modulate the LMP-2-associated signal pathways as reported for HER2- or HER3-affibodies [52,53].

Overall, for the first time, we have produced and characterized four EBV LMP-2-specific affibodies with high affinity and specificity. The affibodies rapidly accumulate in the tumour in EBV LMP-2⁺ tumour xenografts by IV injection. Therefore, the LMP-2-specific affibodies may have great potential for molecular imaging in EBV-associated NPC. Furthermore, PE38KDEL toxin fusion to the $Z_{\text{EBV LMP-2}}$ affibody grants PE38KDEL with specific EBV LMP-2 targeting and cytotoxicity on NPC tumour cells. Since not all EBV-associated tumours express LMP-2, our LMP-2-specific affibodies/affitoxins would be useful for diagnosis or therapeutic treatment of EBV tumours with type II or III latency. Although the established affibody suppresses the tumor growth *in vivo* and the detailed mechanism(s) remains to be investigated, our affitoxin will be a potent anti-NPC drug that might be effective against solid tumors without apparent cytotoxicity to bystander normal cells.

Materials and methods

Design the combined B cell epitopes of LMP-2 for affibody screening

Three B cell epitopes of LMP-2 were predicted and characterized by Xue et al.[54] and the epitopes outside of the LMP-2 transmembrane region from the common C-terminal half of both LMP-2A and LMP-2B were selected for further studies in this report. The selected LMP-2 B-epitopes with the numbers devoted to amino acid residue positions in LMP-2A protein, 199RIEDPPFNSSL209-(GS)-318TLNLT322-(GS)-381KSLSSSTEFIPN391, were linked by glycine-serine (GS) and the codon-optimized nucleotide sequences were then synthesized and cloned at *Bam*H1 and *Hind*III sites of a pET32a(+) vector for expression in *E.coli* BL21 (DE3). The LMP-2 B-epitope fusion protein was verified by SDS-PAGE and Western blot analysis (S1 Fig).

Construction of a phage display library containing staphylococcal protein A (SPA) derived-Z domain scaffold

A combinatorial phage library of the Z domain was prepared as described [30], with random amino acid residues at positions 9, 10, 11, 13, 14, 17, 18, 24, 25, 27, 28, 32 and 35. Briefly, to create the random affibody library, a wild SPA-Z scaffold was used as template for PCR amplification with the random primers from helices 1 and 2 of the Z domain. *Sfi* I/*Not* I digested PCR products were ligated to a pCANTAB5E phagemid vector to construct a recombinant pCANTAB5E/SPA-N vector. *E. coli* TG1 cells were then transformed with the recombinant vector libraries yielding apparent library sizes of a complexity of 1×10^9 and with 100% diversity in SPA-Z scaffold. After evaluated the randomness and capacity of inserted affibody library, the phage stocks then resuspended in sterile PBS/glycerol (20% v/v) solution, finally aliquoted and stored at -80°C . Phage stocks from the obtained libraries by screening were prepared using standard procedures involving M13K07 helper phage.

Phage display selections

Phage selection of the binders to purified bacterial EBV LMP-2 was performed in Immuno tube as described [55]. Briefly, an aliquot of phage stock was thawed and diluted with 9 mL of 2xYT containing 50 $\mu\text{g}/\text{mL}$ of ampicillin and 2% glucose (2xYT-AG). These bacterial cells were infected at $\text{MOI} = 20$ with M13K07 (Invitrogen) and the infected bacteria were incubated in a shaker at 37°C for 2 h. The cells were collected by centrifugation at $1000 \times g$ for 10 min and resuspended in 10 mL of 2xYT containing 100 $\mu\text{g}/\text{mL}$ of ampicillin and 50 $\mu\text{g}/\text{mL}$ of kanamycin. The culture was grown overnight at 37°C before harvesting. Phage-containing cell lysate was clarified by centrifugation at $1000 \times g$ for 20 min. For phage extraction, the lysate was filtered through 0.45 μm filter and concentrated by precipitation with 1/5th volume polyethylene glycol solution (20% PEG 8000, 2.5 M NaCl) for 45min on ice. The precipitated phagemids were centrifuged (20 min, $6000 \times g$, 4°C) and resuspended in 2xYT. The target protein EBV LMP-2 B-epitope (0.45 μM) in 2 ml of carbonate coating buffer per tube was coated on Immuno tube (Greiner Bio-one, Germany) overnight at 4°C , and the unbound protein was removed by PBS containing 0.1% Tween20. After blocking with 5% non-fat milk in PBST for 1 h, the Immuno tubes were incubated with phagemids at 37°C for 2 h. Subsequently, the tubes were washed six times with PBST. The bound phages were eluted with log phase *E. coli* TG1 cells at 37°C for 1 h without shaking. A small aliquot of the infected *E. coli* TG1 culture was ten-fold serially diluted and plated on 2xYT-AG agar plates to determine phage titer. The remaining *E. coli* TG1 culture was then infected with a helper phage M13K07 and subjected to an additional round of screening. In the last cycle, individual bacteria colonies were obtained,

and the culture supernatant derived from the single colony was used for further ELISA screening.

Screening ELISA

An ELISA-based assay was used to further verify their affinities to the target protein LMP-2 according to the methods described by Xue [30]. Briefly, the supernatants (100 μ L) containing potential affibody molecules were loaded in microtiter wells, which had been previously coated with 0.45 μ M (100 μ L/well) LMP-2 B-epitope fusion protein. After blocking and washing, the plates were incubated with 100 μ L of 1:10000 diluted mouse anti-M13 mAb (GE Healthcare, Piscataway, USA) per well for 1 h. After washing the wells four times, the plates were incubated with addition of 100 μ L horseradish peroxidase (HRP) -conjugated goat anti-mouse IgG (1:5,000) per well for 1 h. The wells were washed four times and 3,3',5,5'-Tetramethylbenzidine (TMB) solution was added to each well. After 30 minutes, stop solution (2 M H₂SO₄) was added and the absorbance (OD) at 450 nm was measured in a Bio-tek ELISA microplate reader. The phages with relatively high signal of absorbance value, which bear potential affibody molecules with high affinity to EBV LMP-2, were selected for DNA sequencing and subsequently investigations.

Affibody molecules production

The affibodies selected for further identification were subcloned and generated with C-terminal His-tag fusion proteins for purification. The sequences of selected EBV LMP-2-binding affibody molecules, including Z_{EBV LMP-2 12}, Z_{EBV LMP-2 132}, Z_{EBV LMP-2 137}, Z_{EBV LMP-2 142} (denoted as Z12, Z132, Z137, Z142) and Z_{WT} were separately cloned into a pET21a(+) expression vector in frame with a C-terminal His-tag. *E. coli* BL21(DE3) cells were transformed with the expression plasmids and induced for 4 ~ 6 h at 37°C by 0.8 mM isopropyl-L-thio- β -D-galactopyranoside (IPTG, Sigma-Aldrich Co., St. Louis, MO) for expression of the fusion proteins. The recombinant LMP-2 affibodies with a His-tag at the C-terminus were purified by chromatography with Ni-NTA agarose resin (Qiagen, Hilden, Germany) and verified by SDS-PAGE. The purified proteins were further dialyzed in PBS using Slide-A-Lyzer (Pierce, Rockford, IL, USA) according to the manufacturer's recommendations. After determining concentration using the bicinchoninic acid (BCA) protein quantitation method, the proteins were stored at -80°C for further use.

Surface plasmon resonance analysis

To evaluate the target-binding of the selected Z_{EBV LMP-2} affibodies to EBV LMP-2, surface plasmon resonance (SPR) was performed on a ProteOn XPR36 system (Bio-rad, California, USA). The LMP-2 B-epitope fusion protein (1 nM) served as the ligand was immobilized onto the surface of carboxylate glucans in HTG sensor chip (Bio-rad), as described previously [30,31]. Subsequently, five or six concentrations of each affibody sample were prepared and injected over the chip surface to record sample binding to the surface. All experiments were carried out with a flow rate of 30 μ L/min at 25°C. SPR data sets were fit globally using a 1:1 Langmuir binding model and analyzed by BIA evaluation 3.0.2 software.

Cell culture

EBV⁺ cell lines, including B95-8 (EBV transformed lymphocyte, ATCC: CRL-1612), C666-1 (Human NPC cell line, CVCL_7949) and CNE-2Z (Human NPC cell line, CVCL_6890) were respectively obtained from American Type Culture Collection (ATCC) and Guangzhou Taisheng Bio-Tech Co. Ltd (Guangzhou, China). EBV-negative melanoma cell line of A375

(ATCC: CRL-1619) was obtained from ATCC. The cells were grown in either RPMI-1640 medium (B95-8, C666-1 and CNE-2Z) or high glucose Dulbecco's modified Eagle's medium (DMEM) (A375) supplemented with 10% fetal bovine serum (FBS), 100 units/mL of penicillin, and 0.1 mg/mL streptomycin. All cell lines were maintained by serial passage in 5% CO₂ incubator at 37°C.

Biodistribution of EBV LMP-2 specific affibodies in tumor xenograft mice model

The dynamic distribution and tumor-targeting ability of the EBV LMP-2-specific affibodies were evaluated in nude mice using near-infrared (NIR) optical imaging. 4-week-old female nu/nu (Balb/C) mice were used to establish C666-1 xenograft tumor models. Mice used in this study were purchased from the Shanghai Slac laboratory animal CO. LTD (Shanghai, China). About 4×10^6 cells/100 μ l PBS were subcutaneously inoculated into the scapular region of nude mice. When the tumor volume reached approximately 300 ~ 500 mm³, the mice were used for NIR imaging. EBV LMP-2-specific affibody proteins and Z_{WT} affibody were labelled with Dylight755 molecules (Thermo Fisher Scientific, USA) according to the manufacturer's recommendations. Subsequently, 15.4 nmol of labelled affibody proteins dissolved in 100 μ l PBS were injected via tail vein under isoflurane anesthesia and the imaging was performed using NIR Imaging System (Cri Maestro 2.10, USA) at various time points after injection.

Affitoxin Cloning, expression and purification

The toxin part PE38KDEL [32,56] was connected to the C-terminus of Z142 by a flexible (Gly₄Ser)₃ linker. In brief, the DNA sequence corresponding to PE38KDEL with (Gly₄Ser)₃ linker domain was synthesized and cloned into a vector pET21a (+) between the *EcoRI* and *XhoI* sites to generate the recombinant plasmid pET21a(+)/PE38KDEL. The DNA sequence of Z142 was cloned into the pET21a (+)/PE38KDEL vector between *NdeI* and *EcoRI* sites to generate the recombinant plasmid pET21a (+)/Z_{EBV LMP-2} affitoxin 142. Meanwhile, Z_{WT} was used as a negative control. With the similar method mentioned above, the plasmid of pET21a (+)/Z_{WT} affitoxin was constructed. Finally, two recombinant plasmids were confirmed by DNA sequencing. The expression of Z_{EBV LMP-2} affitoxin 142 (denoted as Z142X) and Z_{WT} affitoxin (denoted as Z_{WT}X) in *E. coli* BL21 (DE3) was induced by 0.8 mM IPTG and verified by SDS-PAGE and Western blot analysis. Then, the fusion proteins were purified by Ni-NTA agarose resin.

Immunofluorescence detection

To determine whether the affibody or affitoxin molecules could bind to the LMP-2 native proteins, IFA was performed as previously described with minor modifications [30,31]. Briefly, EBV⁺ cells, including B95-8, C666-1, CNE-2Z cells and EBV-negative melanoma cells of A375 were seeded in a 24-well plate in 5% CO₂ incubator at 37°C. 24 h later, the medium was replaced with fresh media supplementary with 7.5 μ M affibody or affitoxin molecules or wild Z_{WT} control. After incubation for 6 h, cells were fixed with 4% paraformaldehyde at room temperature (RT) for 10 min. Subsequently, cells were permeabilized by 0.3% Triton X-100 at RT for 10 min followed by blocking with 10% FBS in RPMI-1640. 2 h later, the cells were used for analysis of affibody molecules binding to EBV LMP-2 proteins by mouse anti-His mAb, followed the addition of secondary antibodies FITC-conjugated goat anti-mouse IgG (H+L) (Life Technologies, Carlsbad, CA, USA) for 1 h. Similarly, the cells were used for detection of affitoxin molecules binding to EBV LMP-2 proteins by mouse anti-His mAb, rabbit SPA-Z polyclonal antiserum and mouse PE38KDEL polyclonal antiserum, followed by addition of secondary antibodies FITC-conjugated goat anti-mouse IgG (H+L) or FITC-conjugated goat

anti-rabbit IgG (H+L) (Life Technologies, Carlsbad, CA, USA) at RT for 1 h. The nuclei of cells were counter stained with 50 $\mu\text{g/ml}$ propidium iodide (PI) (Beyotime Biotech Co. Ltd, China) at RT for another 5 min and the fluorescence were observed with a confocal fluorescence microscope (Leica TCS SP2 microscope).

To further confirm the specific binding of LMP-2 specific affibody to native LMP-2, the colocalization was determined in EBV⁺ C666-1 cells by confocal double immunofluorescence assay. The procedure was similar to the above description. Rat anti-LMP-2A mAb (Abcam, Clone 15F9), Cy3-conjugated goat-anti-rat IgG (Beyotime Biotech Co.,Ltd, China) served respectively as the primary and secondary antibody. The nuclei of cells were counter stained with 10 $\mu\text{g/ml}$ Hoechst33342 (Beyotime Biotech Co. Ltd, China).

***In vitro* cytotoxicity efficacy of affitoxin Z142X**

To evaluate the efficacy of Z142X, cell viability assay was performed with Cell Counting kit-8 (CCK-8, Dojindo, Japan) according to the manual provided by the manufacture. Briefly, B95-8, C666-1, CNE-2Z and A375 cells were inoculated in a 96-well plate at 1×10^4 cells/well, followed by incubation with Z142X at different concentrations (0.04, 0.07, 0.14, 0.28, 0.56, 1.11 and 2.22 μM). Cells treated with same concentrations of Z_{WT}X were used as negative controls. Subsequently, the surviving cells were examined respectively after incubation for 0 h, 3 h, 6 h, 12 h, 24 h, 48 h and 72 h using a CCK-8 kit. Absorbance was measured at 450 nm using a microplate reader and cell viability was expressed as a percentage relative to control cells. The half maximal inhibitory concentration (IC₅₀) values were calculated using GraphPad Prism software (GraphPad Software, Inc.).

Mouse acute toxicity assays of affitoxin Z142X

6-week-old BALB/c female mice (n = 4~7 per group) were administered at the indicated doses (55.6, 111, 222, 333, 444, 556, 667 nmol/kg) of Z142X by intravenous tail vein injection. Any reported death cases or moribund conditions that occurred within the 2-week post injection period were taken into consideration. All experiments were performed in triplicate. The lethal dose 50% (LD₅₀) value was calculated by GraphPad Prism 5.0 Software.

Antitumor efficacy of affitoxin Z142X in mouse xenograft tumor models

Therapeutic efficacy of Z142X was evaluated using C666-1 and CNE-2Z tumor-bearing mice. Briefly, 3~4 weeks old BALB/c nude mice were randomly divided into 5 groups (n = 5 for each group). Establishment of C666-1, CNE-2Z and A375 xenograft mouse tumor models have been described as above. Briefly, the tumor was initiated by subcutaneous injection of 4×10^6 cells, which were suspended in 100 μl PBS, into the right scapular region of a nude mouse. When tumor volume reached 50 ~ 100 mm³, the mice were treated with 100 μl Z142X (100 nmol/kg), Z_{WT}X (100 nmol/kg), Z142 (100 nmol/kg), PE38KDEL (100 nmol/kg) or PBS, respectively. The indicated agents were injected every two days for 15 times via tail vein. The therapeutic efficacies and systematic toxicities of affitoxin proteins were assessed based on daily measurements of tumor volume and body weight. Tumor from mice of above five groups were removed and weighed after all treatments and observation period were completed.

Statistical analysis

Data were presented as mean \pm standard deviation (SD). Statistical analysis of the significance between groups was conducted using 2-tailed unpaired Student's test, and $P < 0.05$ was considered to be statistically significant. All calculations were performed with the software SPSS16.0.

Ethics statement

This study was carried out in strict accordance with the Regulations for the Administration of Affairs Concerning Experimental Animals of the State Science and Technology Commission. All animal studies and protocols were approved by the Ethics Committee of Wenzhou Medical University (The permit license number: wydw2017-0504).

Supporting information

S1 Fig. SDS-PAGE (A) and Western blot (B-C) analysis of purified EBV LMP-2 B-epitopes fusion protein. (A) Purified His-tagged LMP-2 B-epitope fusion protein in Coomassie blue staining. (B and C) Western blot of the His-tagged LMP-2 B-epitope fusion protein by a monoclonal anti-His antibody (B) or by the serum of an EBV⁺ NPC patient (C). Two protein extracts were analyzed.

(TIF)

S2 Fig. A representative ELISA screening of LMP-2 binding affibody molecules. The supernatants (100 μ L) containing potential affibody molecules were loaded in microtiter wells, which had been previously coated with 0.45 μ M (100 μ L/well) EBV LMP-2 B-epitope fusion protein. A total of 282 clones from phage display library were screened for its interaction with EBV LMP-2 B-epitope fusion protein by an ELISA assay and the highly (signal intensity) interactive clones to LMP-2 were selected for DNA sequencing to verify of affibody coding.

(TIF)

S3 Fig. Amino acid sequences of the top 4 affibody molecules selected as EBV LMP-2 binders. The amino acid positions 9, 10, 11, 13, 14, 17, 18, 24, 25, 27, 28, 32 and 35 are randomized in the phage display selection. The helical structures are represented in boxes. Horizontal dots indicate the identical amino acid residues in an LMP-2-specific affibody to the amino acid sequences of the original affibody scaffold Z domain (Z_{WT}).

(TIF)

S4 Fig. Representative binding sensorgrams in biosensor assays showed no interaction of the affibody Z142 with immobilized recombinant MAGE-A3. Binding of 1.6, 3.2, 6.4, 12.8, 25.6, 51.2 nM of Z142 Affibody molecule to MAGE-A3 on the sensorchip was analyzed by a SPR-based binding assay.

(TIF)

S5 Fig. Z142X and Z142 inhibit the growth of EBV⁺ B95-8 cells in a concentration-dependent manner. EBV⁺ B95-8 cells in a 96-well plate were treated with various concentrations of Z142X, $Z_{WT}X$, Z142 or PE38KDEL for 72 h. The viability of B95-8 cells decreased along increasing concentration of Z142X and Z142. $Z_{WT}X$ and PE38KDEL displayed only a little or no effect on B95-8 cell viabilities assessed by CCK-8 Kit.

(TIF)

S6 Fig. Z142X kills EBV⁺ cells *in vitro* in a concentration-dependent manner. EBV⁺ cells (B95-8, C666-1 and CNE-2Z) and EBV-negative cells (melanoma A375 cells) in a 96-well plate were treated with various concentrations of Z142X or $Z_{WT}X$ for 72 h. The viability of EBV⁺ cells (B95-8, C666-1 and CNE-2Z cells) decreased along increasing concentration of Z142X, whereas EBV-negative melanoma A375 cells remained fully viable. $Z_{WT}X$ had no effect on any cell lines. Cell viability was assessed using CCK-8 Kit.

(TIF)

S7 Fig. Z142X or other control agents has no tumor-suppressive effect in mice bearing EBV-negative melanoma A375 xenografts. Mice bearing tumors were intravenously injected with 100 nmol/kg Z142X or an equal molar amount of control agents or the same volume of PBS every two days for 15 times via tail vein. Tumor growth was monitored by measuring the tumor volume every day. At the end of the experiment, all tumor grafts were removed and weighed. The control agents (Z_{WTX}, PE38KDEL or PBS) did not show any anti-tumor effect on these mice, nor the Z142X affitoxin and Z142 affibody on tumor growth in mice bearing A375 tumor xenografts. n = 5. 2-tailed unpaired Student's *t* test was used. (TIF)

S1 Table. Kinetic data from the SPR Biosensor Analysis of the Affibody molecules in interaction with LMP-2 B-epitope fusion protein. (DOCX)

S2 Table. The acute toxicity of Z142X affitoxin *in vivo*. (DOCX)

Author Contributions

Conceptualization: Xiangyang Xue, Zhi-Ming Zheng, Lifang Zhang.

Data curation: Shanli Zhu, Lifang Zhang.

Formal analysis: Shanli Zhu, Zhi-Ming Zheng, Lifang Zhang.

Funding acquisition: Lifang Zhang.

Investigation: Shanli Zhu, Jun Chen, Yirong Xiong, Saidu Kamara, Meiping Gu, Wanlin Tang, Shao Chen, Haiyan Dong.

Methodology: Shanli Zhu, Xiangyang Xue, Lifang Zhang.

Project administration: Lifang Zhang.

Resources: Lifang Zhang.

Software: Jun Chen.

Supervision: Xiangyang Xue, Zhi-Ming Zheng, Lifang Zhang.

Validation: Shanli Zhu.

Visualization: Shanli Zhu.

Writing – original draft: Shanli Zhu, Zhi-Ming Zheng, Lifang Zhang.

Writing – review & editing: Shanli Zhu, Zhi-Ming Zheng, Lifang Zhang.

References

1. Thorley-lawson DA, Hawkins JB, Tracy SI, Shapiro M. The Pathogenesis of Epstein-Barr Virus Persistent Infection. *Curr Opin Virol*. 2013; 3(3):227–32. <https://doi.org/10.1016/j.coviro.2013.04.005> PMID: 23683686
2. Young LS, Yap LF, Murray PG. Epstein-Barr virus: more than 50 years old and still providing surprises. *Nat Rev Cancer*. 2016; 16(12):789. <https://doi.org/10.1038/nrc.2016.92> PMID: 27687982
3. Tsao SW, Tsang CM, To KF, Lo KW. The role of Epstein-Barr virus in epithelial malignancies. *J Pathol*. 2015; 235(2):323–333. <https://doi.org/10.1002/path.4448> PMID: 25251730
4. Wolf H, Zur HH, Becker V. EB viral genomes in epithelial nasopharyngeal carcinoma cells. *Nat New Biol*. 1973; 244(138):245–247. <https://doi.org/10.1038/newbio244245a0> PMID: 4353684

5. Pathmanathan R, Prasad U, Sadler R, Flynn K, Raabtraub N. Clonal proliferations of cells infected with Epstein-Barr virus in preinvasive lesions related to nasopharyngeal carcinoma. *N Engl J Med.* 1995; 333(11):693–698. <https://doi.org/10.1056/NEJM199509143331103> PMID: 7637746
6. de Schryver A, Friberg S Jr, Klein G, Henle W, Henle G, De-Thé G, et al. Epstein-Barr virus-associated antibody patterns in carcinoma of the post-nasal space. *Clin Exp Immunol.* 1969; 5(5):443–459. PMID: 4902604
7. Henle W, Henle G, Ho HC, Burtin P, Cachin Y, Clifford P, et al. Antibodies to Epstein-Barr virus in nasopharyngeal carcinoma, other head and neck neoplasms, and control groups. *J Natl Cancer Inst.* 1970; 44(1):225–31. PMID: 11515035
8. Price AM, Luftig MA. To be or not 11b: a multi-step process for Epstein-Barr virus latency establishment and consequences for B cell tumorigenesis. *PLoS Pathog.* 2015; 11(3):e1004656. <https://doi.org/10.1371/journal.ppat.1004656> PMID: 25790223
9. Gewurz BE, Mar JC, Padi M, Zhao B, Shinnars NP, Takasaki K, et al. Canonical NF- κ B Activation Is Essential for Epstein-Barr Virus Latent Membrane Protein 1 TES2/CTAR2 Gene Regulation. *J Virol.* 2011; 85(13):6764–73. <https://doi.org/10.1128/JVI.00422-11> PMID: 21543491
10. Greenfeld H, Takasaki K, Walsh MJ, Ersing I, Bernhardt K, Ma Y, et al. TRAF1 Coordinates Polyubiquitin Signaling to Enhance Epstein-Barr Virus LMP1-Mediated Growth and Survival Pathway Activation. *Plos Pathog.* 2015; 11(5): e1004890. <https://doi.org/10.1371/journal.ppat.1004890> PMID: 25996949
11. Young LS, Rickinson AB. Epstein-Barr virus: 40 years on. *Nat Rev Cancer.* 2014; 4(10): 757–68. <https://doi.org/10.1038/nrc1452> PMID: 15510157
12. Majerciak V, Yang W, Zheng J, Zhu J, Zheng ZM. A Genome-Wide Epstein-Barr Virus Polyadenylation Map and Its Antisense RNA to EBNA. *J Virol.* 2019; 93(2). pii: e01593–18. <https://doi.org/10.1128/JVI.01593-18> PMID: 30355690
13. Longnecker R. Epstein-Barr virus latency: LMP-2, a regulator or means for Epstein-Barr virus persistence? *Adv Cancer Res.* 2000; 79:175–200. [https://doi.org/10.1016/s0065-230x\(00\)79006-3](https://doi.org/10.1016/s0065-230x(00)79006-3) PMID: 10818681
14. Sutkowski N, Chen G, Calderon G, Huber BT. Epstein-Barr virus latent membrane protein LMP-2A is sufficient for transactivation of the human endogenous retrovirus HERV-K18 superantigen. *J Virol.* 2004; 78(14):7852–7860. <https://doi.org/10.1128/JVI.78.14.7852-7860.2004> PMID: 15220463
15. Zhang L, Pagano JS. Interferon regulatory factor 7: a key cellular mediator of LMP-1 in EBV latency and transformation. *Semin Cancer Biol.* 2011; 11(6):445–53. <https://doi.org/10.1006/scbi.2001.0411> PMID: 11669606
16. Pang MF, Lin KW, Peh SC. The signaling pathways of Epstein-Barr virus-encoded latent membrane protein 2A (LMP2A) in latency and cancer. *Cell Mol Biol Lett.* 2009; 14(2):222–247. <https://doi.org/10.2478/s11658-008-0045-2> PMID: 19082921
17. Rechsteiner MP, Berger C, Zauner L, Sigrist JA, Weber M, Longnecker R, et al. Latent membrane protein 2B regulates susceptibility to induction of lytic Epstein-Barr virus infection. *J Virol.* 2008; 82(4):1739–1747. <https://doi.org/10.1128/JVI.01723-07> PMID: 18057232
18. Rovedo M, Longnecker R. Epstein-Barr Virus Latent Membrane Protein 2B (LMP2B) Modulates LMP2A Activity. *J Virol.* 2007; 81(1):84–94. <https://doi.org/10.1128/JVI.01302-06> PMID: 17035319
19. Löfblom J, Feldwisch J, Tolmachev V, Carlsson J, Ståhl S, Frejd FY. Affibody molecules: engineered proteins for therapeutic, diagnostic and biotechnological applications. *FEBS Lett.* 2010; 584(12):2670–2680. <https://doi.org/10.1016/j.febslet.2010.04.014> PMID: 20388508
20. Nord K, Nilsson J, Nilsson B, Uhlén M, Nygren PA. A combinatorial library of an alpha-helical bacterial receptor domain. *Protein Eng.* 1995; 8(6):601–8. <https://doi.org/10.1093/protein/8.6.601> PMID: 8532685
21. Frejd FY, Kim KT. Affibody molecules as engineered protein drugs. *Exp Mol Med.* 2017; 49(3):e306. <https://doi.org/10.1038/emm.2017.35> PMID: 28336959
22. Ståhl S, Gräslund T, Eriksson Karlström A, Frejd FY, Nygren PÅ, et al. Affibody Molecules in Biotechnological and Medical Applications. *Trends Biotechnol.* 2017; 35(8):691–712. <https://doi.org/10.1016/j.tibtech.2017.04.007> PMID: 28514998
23. Andersson KG, Oroujeni M, Garousi J, Mitran B, Ståhl S, Orlova A, et al. Feasibility of imaging of epidermal growth factor receptor expression with ZEGFR:2377 affibody molecule labeled with ^{99m}Tc using a peptide-based cysteine-containing chelator. *Int J Oncol.* 2016; 49(6):2285–2293. <https://doi.org/10.3892/ijo.2016.3721> PMID: 27748899
24. Oroujeni M, Garousi J, Andersson KG, Löfblom J, Mitran B, Orlova A, et al. Preclinical Evaluation of [⁶⁸Ga]Ga-DFO-ZEGFR:2377: A Promising Affibody-Based Probe for Noninvasive PET Imaging of EGFR Expression in Tumors. *Cells.* 2018; 18: 7(9). <https://doi.org/10.3390/cells7090141> PMID: 30231504

25. Orlova A, Magnusson M, Eriksson TL, Nilsson M, Larsson B, Höidén-Guthenberg I, et al. Tumor Imaging Using a Picomolar Affinity HER2 Binding Affibody Molecule. *Cancer Res.* 2006; 66(8):4339–4348. <https://doi.org/10.1158/0008-5472.CAN-05-3521> PMID: 16618759
26. Sörensen J, Velikyan I, Sandberg D, Wennborg A, Feldwisch J, Tolmachev V, et al. Measuring HER2-Receptor Expression In Metastatic Breast Cancer Using [68Ga]ABY-025 Affibody PET/CT. *Theranostics.* 2016; 6:262–71. <https://doi.org/10.7150/thno.13502> PMID: 26877784
27. Malm M, Kronqvist N, Lindberg H, Gudmundsdottir L, Bass T, Frejd FY, et al. Inhibiting HER3-Mediated Tumor Cell Growth with Affibody Molecules Engineered to Low Picomolar Affinity by Position-Directed Error-Prone PCR-Like Diversification. *Plos One.* 2013; 8: e62791. <https://doi.org/10.1371/journal.pone.0062791> PMID: 23675426
28. Schardt JS, Oubaid JM, Williams SC, Howard JL, Aloimonos CM, Bookstaver ML, et al. Engineered Multivalency Enhances Affibody-Based HER3 Inhibition and Downregulation in Cancer Cells. *Mol Pharm.* 2017; 14:1047–1056. <https://doi.org/10.1021/acs.molpharmaceut.6b00919> PMID: 28248115
29. Fedorova A, Zobel K, Gill HS, Ogasawara A, Flores JE, Tinianow JN, et al. The Development of Peptide-Based Tools for the Analysis of Angiogenesis. *Chem Biol.* 2011; 18(7):839–845. <https://doi.org/10.1016/j.chembiol.2011.05.011> PMID: 21802005
30. Xue X, Wang B, Du W, Zhang C, Song Y, Cai Y, et al. Generation of affibody molecules specific for HPV16 E7 recognition. *Oncotarget.* 2016; 7(45):73995. <https://doi.org/10.18632/oncotarget.12174> PMID: 27659535
31. Zhu S, Zhu J, Song Y, Chen J, Wang L, Zhou M, et al. Bispecific affibody molecule targeting HPV16 and HPV18E7 oncoproteins for enhanced molecular imaging of cervical cancer. *Appl Microbiol Biotechnol.* 2018; <https://doi.org/10.1007/s00253-018-9167-2> PMID: 29938318
32. Kreitman RJ, Pastan I. Importance of the glutamate residue of KDEL in increasing the cytotoxicity of *Pseudomonas* exotoxin derivatives and for increased binding to the KDEL receptor. *Biochem J.* 1995; 307 (Pt 1):29–37.
33. Michalska M, Wolf P. *Pseudomonas* Exotoxin A: optimized by evolution for effective killing. *Front Microbiol.* 2015; 6:963. <https://doi.org/10.3389/fmicb.2015.00963> eCollection 2015. PMID: 26441897
34. Mazor R, Onda M, Pastan I. Immunogenicity of therapeutic recombinant immunotoxins. *Immunol Rev.* 2016; 270(1):152–64. <https://doi.org/10.1111/imr.12390> PMID: 26864110
35. Torre LA, Bray F, Siegel RL, Ferlay J, Lortet-Tieulent J, Jemal A. Global cancer statistics, 2012. *CA Cancer J Clin.* 2015; 65(2):87–108. <https://doi.org/10.3322/caac.21262> PMID: 25651787
36. Chia WK, Teo M, Wang WW, Lee B, Ang SF, Tai WM, et al. Adoptive T-cell Transfer and Chemotherapy in the First-line Treatment of Metastatic and/or Locally Recurrent Nasopharyngeal Carcinoma. *Mol Ther.* 2014; 22(1):132–139. <https://doi.org/10.1038/mt.2013.242> PMID: 24297049
37. Chen MY, Jiang R, Guo L, Zou X, Liu Q, Sun R, et al. Locoregional radiotherapy in patients with distant metastases of nasopharyngeal carcinoma at diagnosis. *Chin J Cancer.* 2013; 32(11):604–613. <https://doi.org/10.5732/cjc.013.10148> PMID: 24206918
38. Niedobitek G, Hansmann ML, Herbst H, Young LS, Dienemann D, Hartmann CA, et al. Epstein-Barr virus and carcinomas: undifferentiated carcinomas but not squamous cell carcinomas of the nasopharynx are regularly associated with the virus. *J Pathol.* 1991; 165(1):17–24. <https://doi.org/10.1002/path.1711650105> PMID: 1659626
39. Longnecker R, Kieff E. A second Epstein-Barr virus membrane protein (LMP2) is expressed in latent infection and colocalizes with LMP1. *J Virol.* 1990; 64(5):2319–26. PMID: 2157888
40. Tomaszewski-flick MJ, Rowe DT. Minimal protein domain requirements for the intracellular localization and self-aggregation of Epstein-Barr virus latent membrane protein 2. *Virus Genes.* 2007; 35(2):225–234. <https://doi.org/10.1007/s11262-007-0118-8> PMID: 17564822
41. Feldwisch J, Tolmachev V. Engineering of affibody molecules for therapy and diagnostics. *Methods Mol Biol.* 2012; 899:103–126. https://doi.org/10.1007/978-1-61779-921-1_7 PMID: 22735949
42. Mitran B, Altai M, Hofström C, Honarvar H, Sandström M, Orlova A, et al. Evaluation of 99mTc-Z IGF1R:4551-GGFC affibody molecule, a new probe for imaging of insulin-like growth factor type 1 receptor expression. *Amino acids.* 2015; 47(2):303–15. <https://doi.org/10.1007/s00726-014-1859-z> PMID: 25425114
43. Wikman M, Rowcliffe E, Friedman M, Henning P, Lindholm L, Olofsson S, et al. Selection and characterization of an HIV-1 gp120-binding affibody ligand. *Biotechnol Appl Biochem.* 2006; 45(Pt 2):93–105. <https://doi.org/10.1042/BA20060016> PMID: 16712522
44. Sörensen J, Sandberg D, Sandström M, Wennborg A, Feldwisch J, Tolmachev V, et al. First-in-human molecular imaging of HER2 expression in breast cancer metastases using the 111In-ABY-025 affibody molecule. *J Nucl Med.* 2014; 55(5):730–5. <https://doi.org/10.2967/jnumed.113.131243> PMID: 24665085

45. Cheng Q, Wällberg H, Grafström J, Lu L, Thorell JO, HäggOlofsson M, et al. Preclinical PET imaging of EGFR levels: pairing a targeting with a non-targeting Sel-tagged Affibody-based tracer to estimate the specific uptake. *EJNMMI Res.* 2016; 6(1):58. <https://doi.org/10.1186/s13550-016-0213-8> PMID: 27388754
46. Oroujeni M, Garousi J, Andersson KG, Löfblom J, Mitran B, Orlova A, et al. Preclinical Evaluation of [68Ga]Ga-DFO-ZEGFR:2377: A Promising Affibody-Based Probe for Noninvasive PET Imaging of EGFR Expression in Tumors. *Cells.* 2018; 7(9). pii: E141. <https://doi.org/10.3390/cells7090141> PMID: 30231504
47. Rosestedt M, Andersson KG, Mitran B, Tolmachev V, Löfblom J, Orlova A, et al. Affibody-mediated PET imaging of HER3 expression in malignant tumours. *Sci Rep.* 2015; 5:15226. <https://doi.org/10.1038/srep15226> PMID: 26477646
48. Baum RP, Prasad V, Müller D, Schuchardt C, Orlova A, Wennborg A, et al. Molecular imaging of HER2-expressing malignant tumors in breast cancer patients using synthetic 111In- or 68Ga-labeled affibody molecules. *J Nucl Med.* 2010; 51(6):892–897. <https://doi.org/10.2967/jnumed.109.073239> PMID: 20484419
49. Zielinski R, Lyakhov I, Jacobs A, Chertov O, Kramer-Marek G, Francella N, et al. Affitoxin- A Novel Recombinant, HER2-Specific, Anti-Cancer Agent for Targeted Therapy of HER2-Positive Tumors. *J Immunother.* 2009; 32(8):817–25. <https://doi.org/10.1097/CJI.0b013e3181ad4d5d> PMID: 19752752
50. Zielinski R, Lyakhov I, Hassan M, Kuban M, Shafer-Weaver K, Gandjbakhche A, et al. HER2-Affitoxin: A Potent Therapeutic Agent for the Treatment of HER2-Overexpressing Tumors. *Clin Cancer Res.* 2011; 17(15):5071–5081. <https://doi.org/10.1158/1078-0432.CCR-10-2887> PMID: 21791637
51. Iglewski BH, Liu PV, Kabat D. Mechanism of action of *Pseudomonas aeruginosa* exotoxin A adenine diphosphate ribosylation of mammalian elongation factor 2 in vitro and in vivo. *Infect Immun.* 1977; 15:138–144. PMID: 188760
52. Ekerljung L, Lindborg M, Gedda L, Frejd FY, Carlsson J, Lennartsson J. Dimeric HER2-specific affibody molecules inhibit proliferation of the SKBR-3 breast cancer cell line. *Biochem Biophys Res Commun.* 2008; 377(2):489–494. <https://doi.org/10.1016/j.bbrc.2008.10.027> PMID: 18930032
53. Göstring L, Malm M, Höiden-Guthenberg I, Frejd FY, Ståhl S, Löfblom J, et al. Cellular effects of HER3-specific affibody molecules. *PLoS One.* 2012; 7(6):e40023. <https://doi.org/10.1371/journal.pone.0040023> PMID: 22768204
54. Xue X, Zhu S, Li W, Chen J, Ou Q, Zheng M, et al. Identification and characterization of novel B-cell epitopes within EBV latent membrane protein 2 (LMP2). *Viral Immunol.* 2011; 24(3):227–236. <https://doi.org/10.1089/vim.2010.0092> PMID: 21668364
55. Aavula SM, Nimmagadda SV, Biradhar N, Sula S, Chandran D, Lingala R, et al. Generation and Characterization of an scFv Directed against Site II of Rabies Glycoprotein. *Biotechnol Res Int.* 2011; 2011:652147. <https://doi.org/10.4061/2011/652147> PMID: 22007309
56. Song S, Xue J, Fan K, Kou G, Zhou Q, Wang H, et al. Preparation and characterization of fusion protein truncated *Pseudomonas* Exotoxin A (PE38KDEL) in *Escherichia coli*. *Protein Expr Purif.* 2005; 44(1):52–7. <https://doi.org/10.1016/j.pep.2005.04.004> PMID: 15922623